



**HAL**  
open science

## A new all-metal induction furnace for noble gas extraction

Laurent Zimmermann, Guillaume Avice, Pierre-Henri Blard, Bernard Marty, Evelyn Füre, Peter G Burnard

► **To cite this version:**

Laurent Zimmermann, Guillaume Avice, Pierre-Henri Blard, Bernard Marty, Evelyn Füre, et al.. A new all-metal induction furnace for noble gas extraction. *Chemical Geology*, 2018, 480, pp.86-92. 10.1016/j.chemgeo.2017.09.018 . hal-03749821

**HAL Id: hal-03749821**

**<https://hal.science/hal-03749821>**

Submitted on 11 Aug 2022

**HAL** is a multi-disciplinary open access archive for the deposit and dissemination of scientific research documents, whether they are published or not. The documents may come from teaching and research institutions in France or abroad, or from public or private research centers.

L'archive ouverte pluridisciplinaire **HAL**, est destinée au dépôt et à la diffusion de documents scientifiques de niveau recherche, publiés ou non, émanant des établissements d'enseignement et de recherche français ou étrangers, des laboratoires publics ou privés.

1                   Development of a new full-metal induction furnace for  
2                   noble gas extraction

3  
4  
5   Laurent ZIMMERMANN Laurent <sup>\* a</sup>, Guillaume AVICE <sup>a,b</sup>, Pierre-Henri BLARD <sup>a</sup>,  
6   Bernard MARTY <sup>a</sup>, Evelyn FÜRI <sup>a</sup> and Peter G. BURNARD <sup>a</sup>

7  
8   <sup>a</sup> Centre de Recherches Pétrographiques et Géochimiques, UMR7358, CNRS -  
9   Université de Lorraine, BP20, 54501 Vandoeuvre-lès-Nancy Cedex, France

10   <sup>b</sup> California Institute of Technology, Division of Geological and Planetary Sciences,  
11   Pasadena, CA91125, USA

12   \* Corresponding author e-mail: [laurentz@crpg.cnrs-nancy.fr](mailto:laurentz@crpg.cnrs-nancy.fr)

13  
14   Keywords: Noble gases; extraction, full-metal induction furnace, low blank

15  
16   Abstract

17           Noble gases (He, Ne, Ar, Kr, Xe) are excellent geochemical tracers of volatile  
18   origins and geochemical processes between the main terrestrial reservoirs (mantle,  
19   crust, atmosphere). As inert elements they are affected by physical phenomena such  
20   as supply of volatile elements to the Earth, degassing and subduction into the Earth's  
21   mantle.

22           Producing accurate and valuable data from geological samples is often a  
23   challenge for scientists, since it requires a mass spectrometer with a very good  
24   resolution and sensitivity to measure noble gases, a purification line to purify them,  
25   and especially a heating system to efficiently extract them from the minerals with  
26   negligible blank amounts

27 We have developed at the CRPG a new full-metal induction furnace to extract,  
28 in vacuum, all noble gases from minerals typically analysed in geochemical  
29 laboratories such as pyroxene, olivine, quartz or barite.

30 The grain(s), 125 to 3000  $\mu\text{m}$  in size, are packed into a metallic foil and loaded  
31 onto a carousel before their analysis. The Sample, with a mass of up to 1 g are then  
32 sequentially dropped into a Ta-crucible, which has previously been degassed. Only 3  
33 minutes are necessary to reach a temperature of  $> 1500^\circ\text{C}$  inside the crucible.  
34 Helium and neon are easily extracted from pyroxene and olivine at  $1770^\circ\text{C}$ , as well  
35 as from quartz at  $1500^\circ\text{C}$ . Heavy noble gases are extracted at  $> 1700^\circ\text{C}$  from the  
36 same minerals. Noble gas blanks, measured under the same analytical conditions as  
37 the samples are extremely low:  $1.64 \times 10^{-15}$  mole  $^4\text{He}$ ,  $5.80 \times 10^{-17}$  mole  $^{20}\text{Ne}$ ,  $2.13 \times$   
38  $10^{-18}$  mole  $^{84}\text{Kr}$  and  $4.81 \times 10^{-18}$  mole  $^{132}\text{Xe}$ . Hence, our new furnace represents a  
39 powerful tool for the noble gas extraction from small sample amounts and/or gas-  
40 poor minerals, with the capacity of targeting even the most refractory phases.

41

42 1/ Introduction

43

44 Due to their chemical inertness, noble gases are mostly impacted by physical  
45 processes such as phase changes and nuclear reactions, and they constitute a  
46 powerful set of geochemical and cosmochemical tracers (Ozima and Podosek,  
47 2002). Several isotopes of noble gases are produced by nuclear reactions such as  
48 radioactive decay (e.g.  $^{40}\text{K}$  to  $^{40}\text{Ar}$  or  $^{129}\text{I}$  to  $^{129}\text{Xe}$ ), and spontaneous fission (e.g.  $^{238}\text{U}$   
49 to  $^{131-136}\text{Xe}$ ). Various noble gas isotopes are also the final products of interactions  
50 between cosmic rays and Earth's surface material (e.g., through spallation reactions  
51 on Mg,Si, Fe to cosmogenic  $^3\text{He}$  and  $^{21}\text{Ne}$ ). In such a case, cosmic ray-produced

52 isotopes can be used to derive surface exposure ages (e.g. Blard et al., 2014).  
53 Meteoritic noble gases permit to establish the exposure duration of meteorite parent  
54 bodies in space using cosmogenic isotopes to explore the origin of solar system  
55 matter, and to investigate the genetic relationships between planetary reservoirs (Ott  
56 1988).

57         The determination of the noble gas composition of rocks and minerals requires  
58 four main steps: extraction, purification, separation and analysis of a pure noble gas  
59 fraction (Wieler et al. 2014). Each step is critical for ensuring that: (i) all noble gases  
60 have been extracted from the sample; (ii) the gas fraction does not contain other  
61 chemicals known to create isobaric interferences with noble gas isotopes (e.g.  $^1\text{H}^{35}\text{Cl}$   
62 with  $^{36}\text{Ar}$ ,  $^{44}\text{CO}_2^{++}$  with  $^{22}\text{Ne}$ ); (iii) noble gases are well separated and do not compete  
63 with each other in the ion source and (iv) the mass spectrometer is well tuned to  
64 ensure accurate and precise results.

65         Generally, the amount of noble gases in rocks is extremely small, typically of  
66 the order of the femtomole. In addition, the blank, that is the amount of noble gases  
67 degassed by the analytical system, must be much lower than the sample. A major  
68 source of blank noble gases is the extraction system. In order to get a sufficient  
69 signal, several tens to hundreds of mg of sample are often necessary. Such amounts  
70 are generally heated sequentially in a furnace (stepwise heating). However, noble  
71 gas degassing of the inner part of the furnace increases drastically with temperature,  
72 and can overcome the signal of the the sample at high temperature (i.e., 1600°C and  
73 over) for gas-poor rocks and minerals

74         In this paper, we present the conceptual design and the technical details of an  
75 Ultra-High Vacuum (UHV) full metal induction furnace, which was conceived, built,  
76 and developed at CRPG, (Nancy, France). This new apparatus permits to extract, by

77 fusion, more than 99% of noble gases (He, Ne, Ar, Kr and Xe) contained in minerals  
78 such as quartz, pyroxene, olivine, barite or sulfide, with negligible blank amounts.  
79 This furnace is easy to use, safe, efficient and robust.

80

81 2/ Description of the furnace

82

83 2.1/Design of the vacuum vessel

84

85 The furnace vacuum vessel is mainly composed of two CF160 flanges. A  
86 CF40 flange, welded onto the upper part, permits to connect the vacuum vessel to a  
87 carrousel containing samples and to the purification line. A pyrex viewport is also  
88 connected to this flange in order to allow monitoring the temperature of the crucible  
89 with an optical pyrometer. A funnel has been machined into the CF160 flange to  
90 guide samples toward the Ta crucible. The top flange is cooled by water circulating  
91 through the metallic disk N°1 (Figure 1). A double wall was welded on the second  
92 CF160 flange in order to cool the lateral surface of the furnace. A second metallic  
93 disk (metallic disk N°2) was welded onto this double wall to cool the entire inner  
94 surface (Figure 1).

95 A 15 cm<sup>3</sup> crucible containing the sample, made of tantalum (Neyco Company<sup>®</sup>,  
96 LTA15CC) is heated by induction. It is maintained in the middle of the vacuum vessel  
97 by a ceramic holder (Figure 1).

98 A quartz cylinder enclosing the crucible protects the induction coil and the  
99 inner surface of the furnace against condensable species such as Al and Sn from the  
100 metallic foils and carbon, chlorides, sulphides released upon heating of the minerals  
101 (Figure 2).

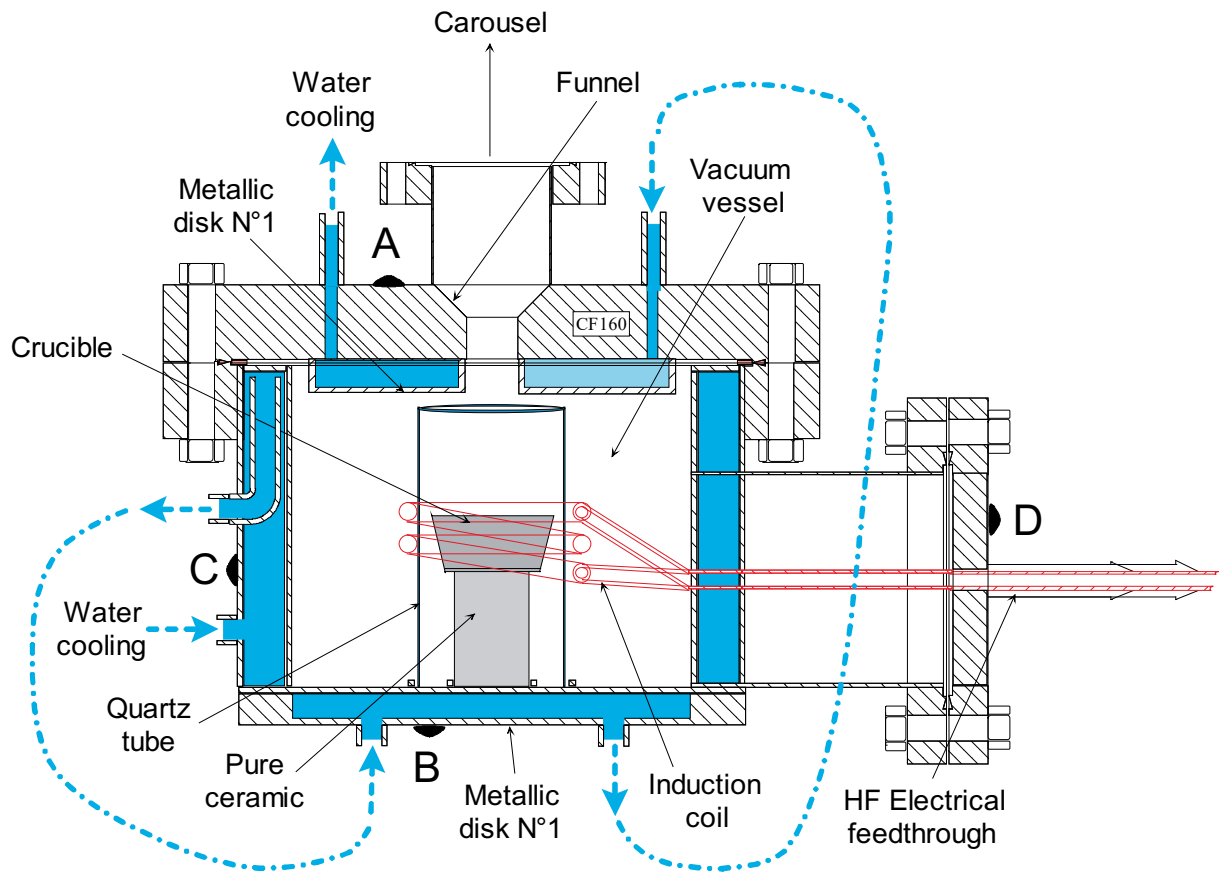
102           The induction coil is placed around the quartz tube. It is connected to a high  
103 frequency (HF) electrical feedthrough cooled by a water circulation. This coil has  
104 been adapted to the geometry of the tantalum crucible in order to optimize the  
105 heating.

106           Because the inner volume of the furnace is important ( $\approx 2100 \text{ cm}^3$ ), we  
107 recommend using a cryogenic trap outside the furnace to concentrate noble gases  
108 into a smaller volume of the purification line.

109           During extraction, two fans are used to cool the external HF connexion of the  
110 furnace. One of the fans is used to cool the ceramics of the HF electrical  
111 feedthrough, while the second one cools the CF63 flange. A triple water cooling  
112 system ( $\approx 60 \text{ l.h}^{-1}$ ) passing through the top CF160 flange, the vertical wall of the  
113 vessel and the bottom metal disk is cooling the inner surface (Figure 3). The  
114 temperature, measured at points A, B, and C (Figure 1), remains below  $30^\circ\text{C}$  after a  
115 heating duration of 20 minutes at  $1800^\circ\text{C}$  of the crucible. The temperature of the  
116 CF63 flange can reach up to  $50^\circ\text{C}$  (point D, Figure 1).

117           The samples are packed into a metallic foil (Sn, Al or Cu) of high purity  
118 (99.99%). They are stored in a metal carrousel connected to the upper part of the  
119 furnace.

120

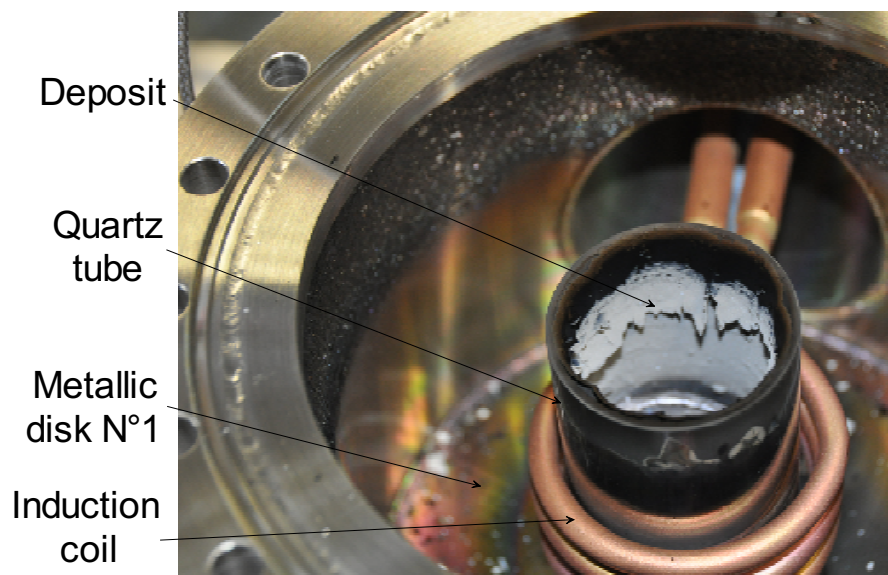


121

122

123 Figure 1: Schematic diagram of the full metal induction furnace showing the induction  
 124 coil with the tantalum crucible and the triple water circulation used to cool the inner  
 125 surface of the vacuum vessel.

126

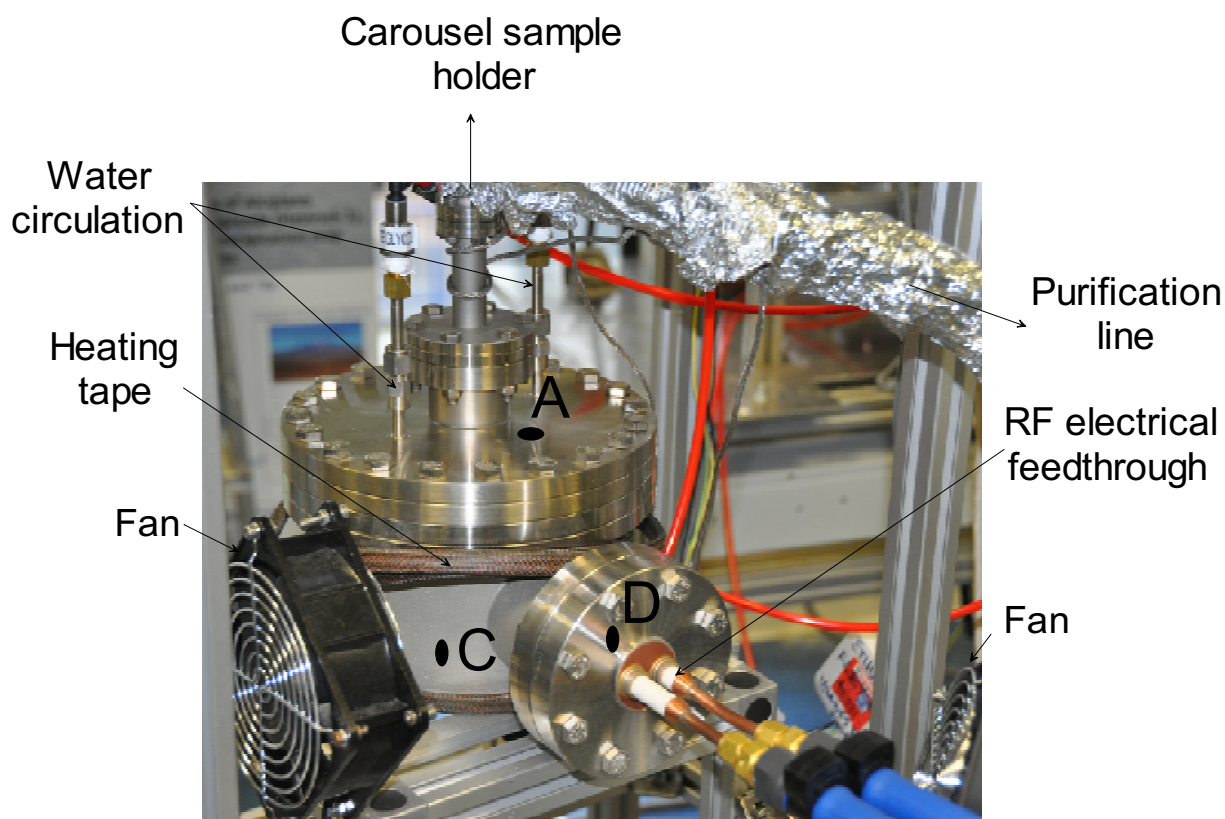


127

128

129 Figure 2: Detailed view of the bottom part of the furnace. The distance between the  
130 top of the quartz tube and the top CF160 flange has been reduced to 2 mm in order  
131 to favour deposits of carbon, sulphides and chlorides on the inner surface of the  
132 quartz tube. Secondary deposits can be observed on the top part of the double wall.  
133 They represent less than 5 % wt of the total deposits.

134



135

136

137 Figure 3: External view of the all-metal induction furnace. A heating tape around the  
138 vacuum vessel bakes the furnace until up to 200°C to desorb atmospheric gases  
139 from the inner surfaces. After one night of baking under vacuum, the pressure ( $5 \times$   
140  $10^{-9}$  mbar) is compatible with the requirements for noble gas measurements. Three  
141 water circulations, connected by red plastic tubes, cool the inner walls during an  
142 extraction.

143

144 2.2/ Nature of the materials

145

146 The choice of the materials used for noble gas extraction systems is critical to  
147 ensure good thermal, electrical and mechanical properties, to prevent contaminations  
148 (e.g., chemicals, manufacturing residues), and to ensure low noble gas blanks.

149 Although several refractory metals such as molybdenum ( $T_{\text{melt}} = 2623^{\circ}\text{C}$ ),  
150 tantalum ( $T_{\text{melt}} = 3020^{\circ}\text{C}$ ) or platinum ( $T_{\text{melt}} = 1768^{\circ}\text{C}$ ) can be used for the crucible,  
151 we recommend tantalum because it yields low helium blanks. For example, during an  
152 extraction at  $1500^{\circ}\text{C}$  with a double-vacuum high temperature furnace, helium blanks  
153 with a Ta crucible were  $9 \times 10^{-15}$  mole  $^4\text{He}$ , whereas blanks analysed under the same  
154 analytical conditions but using a Mo crucible were higher by a factor 8 ( $4 \times 10^{-14}$  mole  
155  $^4\text{He}$ ). Tantalum presents also very low blanks for Kr and Xe despite the formation of  
156 alloys with elements such as Al and Sn, that are parts of the metallic foils used to  
157 pack samples. Such alloys can increase heavy noble gas blanks by a factor 3  
158 (Niedermann et al. 1997).

159 Preliminary tests revealed high Ar blanks ( $> 10^{-10}$  mole of  $^{40}\text{Ar}$ ) at  $1700^{\circ}\text{C}$  with  
160 an isotopic composition similar to that of air. This contamination is likely due to the  
161 manufacturing method of the crucible (e.g. if pure argon is used to avoid oxidation of  
162 tantalum at high temperature). To resolve this issue, we are exploring other  
163 commercial suppliers.

164 Nitrogen measurements remain to be developed with this induction furnace.  
165 For N analysis, Mo or Ta crucibles should be avoided because these refractory  
166 metals are known to chemically react with nitrogen (Yokochi et al. 2006). Platinum,

167 despite its low melting temperature (1768°C) and high cost, seems more appropriate  
168 for this purpose.

169 The crucible sits on an ultra-pure ceramic ( $\text{Al}_2\text{O}_3$ ). This material has been  
170 chosen because it does not melt at the maximum temperature of the furnace ( $t_{\text{melt}} =$   
171 2030°C). Furthermore, it tolerates brutal temperature variations ( $> 400 \text{ }^\circ\text{C}\cdot\text{min}^{-1}$ )  
172 without damage and its noble gas degassing rate at high temperature is low. A visual  
173 control of this is usually done after opening the furnace to ensure its physical  
174 integrity.

175 The vacuum chamber of the furnace is made of stainless steel (304L and  
176 316LN). This material is easily to weld and has a negligible helium permeability,  
177 compared to the other induction furnaces made of glass for example (Marty et al.  
178 1995).

179

### 180 2.3/ Furnace cleaning operations

181

182 Before the first operation, the furnace was cleaned before the first operation in  
183 three ultrasonic baths for 2-3 hours each in Decon90, a detergent used to eliminate  
184 up to 99.95% of hydrocarbons present on the metallic surfaces (Chiggiato et al.  
185 1999). The vacuum chamber was systematically rinsed with deionized water after  
186 each bath. Finally, the furnace was dried in an oven at 100-110°C. We recommend  
187 cleaning the furnace after the analyses of 20-30 samples in order to remove  
188 condensates on the inner surfaces of the furnace. 90% to 95% condensates are  
189 usually present on the inner surfaces of the quartz cylinder. This inexpensive  
190 component is systematically replaced at each cleaning operation. Deposits observed  
191 on the top part of the furnace (Figure N°2), namely less than 5 % by mass of the

192 condensed species, are eliminated by suction. The tantalum crucible can be used  
193 several times, despite the crystallization traces at its surface because: (i) These  
194 traces have no effects on its thermal and mechanical properties and (ii) this  
195 phenomenon has not effect on the noble gas blanks. We also checked the crucible  
196 under the microscope after high temperature extraction of noble gases from olivine  
197 and pyroxene. The crucible was re-cristallized and corroded due to chemical  
198 reactions with the melts. We therefore recommend replacind it after 40-80 analytical  
199 cycles.

200

#### 201 2.4/ Thermal properties

202

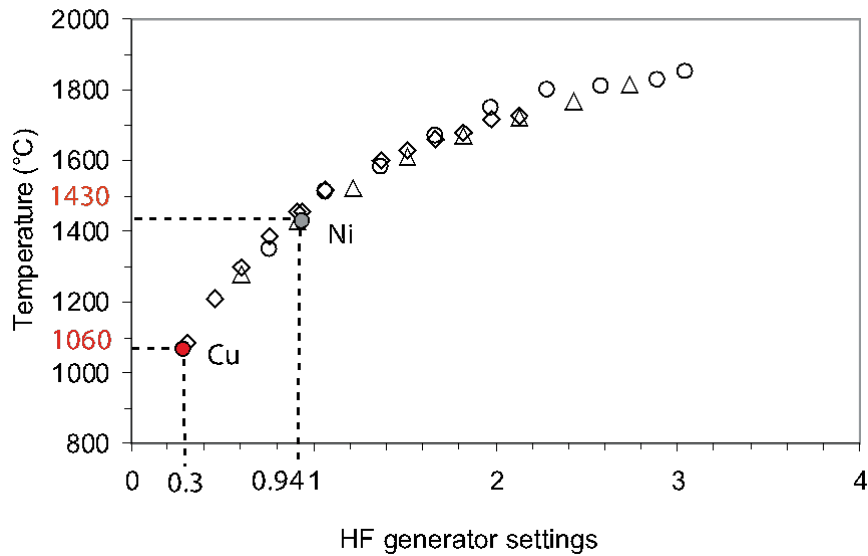
203 The temperature of the tantalum crucible is measured through a pyrex  
204 viewport, connected to the top CF 200 flange (Figure 1), using an optical pyrometer  
205 ((Impac<sup>®</sup>, pyrometer IS-2). Measurements of the temperatures, ranging from 900°C  
206 to 1900°C, have been used to determine a precise calibration curve between the  
207 temperature of the crucible and the power settings of the HF generator. Five minutes  
208 between each temperature step were necessary to ensure temperature stability.  
209 These tests were conducted three times (open triangle circle and diamond symbols  
210 in (Figure 4) and show a good reproducibility. Temperature estimates have also been  
211 verified by melting two pure metals: a Cu and a Ni foil (red and grey circle, Figure 4).  
212 These metals were melted at the observed temperatures of 1060°C and 1430°C for  
213 Cu and Ni, respectively which are in good agreement with the true melting  
214 temperatures (1064°C and 1455°C for Cu and Ni, respectively, Handbook of  
215 Chemistry and Physics).

216 In the range of 580°C-900°C, temperatures were not measured but a reddish  
217 glow of the crucible was observed and the temperatures were estimated from the  
218 calibration curve. Extrapolating the temperature below this range is difficult but the  
219 pressure increase from  $4 \times 10^{-9}$  mbar to  $2 \times 10^{-7}$  mbar indicates heating of the  
220 crucible.

221 The heating tests revealed that the tantalum crucible weighing 120 g was  
222 efficiently heated up to 1800°C, in good agreement with the high temperatures  
223 (>1500°C) obtained with other induction furnaces (Marty et al. 1995, Chennaoui-  
224 Aoudjehane, 1992). For each step, the temperature is stable within ~ 1% (Figure 5).  
225 Possible electric and thermal constraints during heating are likely to be minimal  
226 because the crucible is not attached to the vessel. Thanks to this arrangement,  
227 temperatures higher than 1500°C can be achieved within ~ 3 minutes without any  
228 risks of damage. The heating rate ( $400^\circ\text{C}\cdot\text{min}^{-1}$  on average), is thus improved by a  
229 factor of 5 to 10 compared to those obtained with other double-vacuum high  
230 temperature furnaces (Staudacher et al. 1978; Maruoka et Matsuda, 2001; Aciego et  
231 al. 2007). The cooling rates are also fast (close to  $300^\circ\text{C}\cdot\text{min}^{-1}$  for 500°C to 1500°C  
232 temperature steps) because the crucible, with a weight of only 120 g, has a low  
233 thermal inertia. These technical characteristics are major assets to minimize noble  
234 gas blanks, reduce the duration of extraction, as well as to diminish the amounts of  
235  $\text{H}_2$  produced upon heating.

236 The induction coil has been adapted to the geometry of the tantalum crucible  
237 to increase the efficiency of the heating so that the thermal loss by conduction is  
238 minimized thanks to the low thermal conductivity ( $\approx 3\text{-}5 \text{ W}\cdot\text{m}^{-1}\cdot\text{K}^{-1}$  at 1000°C) of the  
239 ceramic that supports the crucible.

240

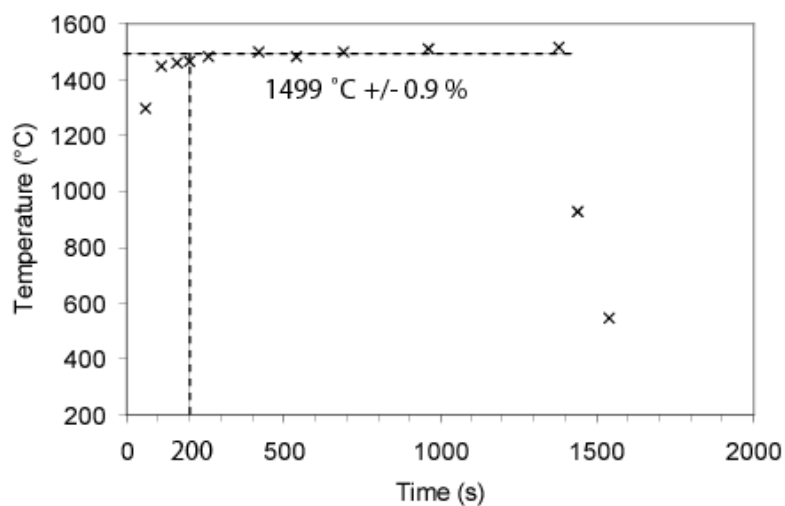


241

242

243 Figure 4: Evolution of the temperature (°C) as a function of the HF generator settings  
 244 between 1000°C and 1500°C. The thermal loss by radiation of the crucible above  
 245 1500°C reduces the heating efficiency. The induction furnace has been tested up to  
 246 1850°C with the HF generator adjusted to 50% maximum power. We think that it will  
 247 be possible to further increase the temperature up to 2000°C.

248



249

250 Figure 5: Measurements of the temperature showing the good thermal stability of the  
 251 furnace, here 1499°C +/- 0.9%. The temperature was stabilized after 200 seconds.

252

253 3/ Analytical procedure

254

255 Nineteen samples were cleaned in acetone in an ultrasonic bath for 5 minutes,  
256 packed into a Sn or Al foil, and loaded into a carousel connected at the upper part of  
257 the induction furnace. The carousel and the furnace chamber were then pumped  
258 and baked at 200°C for 12-14 hours. Measurements of neon have shown that the Ne  
259 blanks were decreased by a factor 40 after baking. The electric power passing  
260 through the induction coil was increased, and the temperature was monitored with an  
261 optical pyrometer. Minerals such as pyroxenes and olivines were melted under static  
262 vacuum at 1700-1800°C for 10 minutes. The temperature of the crucible was then  
263 decreased to room temperature in order to reduce the H<sub>2</sub> pressure produced by hot  
264 tantalum.

265 Helium and neon were purified using two charcoal traps held at 77K for 10  
266 minutes each in order to trap argon degassed by the crucible (see description above)  
267 and three titanium sponge getters (Johnson Matthey®, mesh m3N8 t2N8) for 10  
268 minutes at room temperature. The two noble gases were then separated using a  
269 cryogenic trap held at 10K. Krypton and Xenon were purified using several getters  
270 and a glass finger to trap them at 77K. Argon trapped during this step (≈ 5 %) was  
271 eliminated through several cycles of heating-cooling of the glass tube between 77K  
272 and 300K. 95 % of the argon was desorbed at each cycle and pumped out. The Kr-  
273 Xe fraction was completely separated from argon after three cycles. The whole  
274 purification line was maintained at 320K to avoid adsorption of the heavy noble gases  
275 onto the inner surfaces. Notably, this temperature does not affect the noble gas  
276 blanks. The abundances of the noble gases in the samples were determined with a

277 mass spectrometer operating in static mode and calibrated through noble gas  
278 standards.

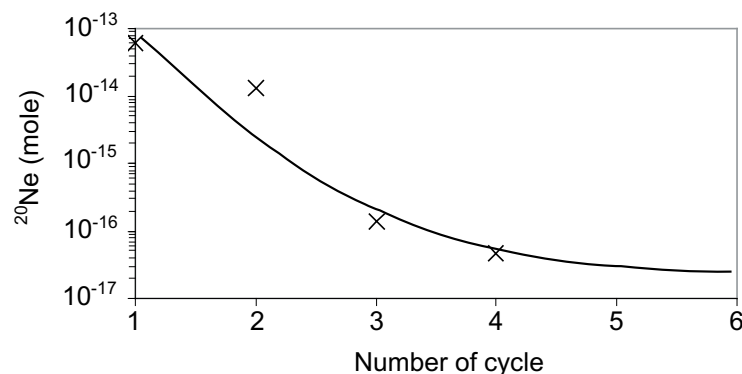
279

280 4/ Furnace blank

281

282 After baking of the furnace for 12 hours at 200°C, the main source of the noble  
283 gas blanks in the furnace is the crucible, especially in the high temperature range  
284 above 1500°C. The crucible was thus degassed during several cycles at 1800°C-  
285 1850°C while pumping. The number and the duration of each cycle depends of the  
286 targeted noble gases, namely only 1 cycle of 30 minutes for He and 3-4 cycles of 60  
287 minutes for Ne, Kr and Xe. Between each cycle, blanks were analysed to check their  
288 evolution (Figure 6).

289



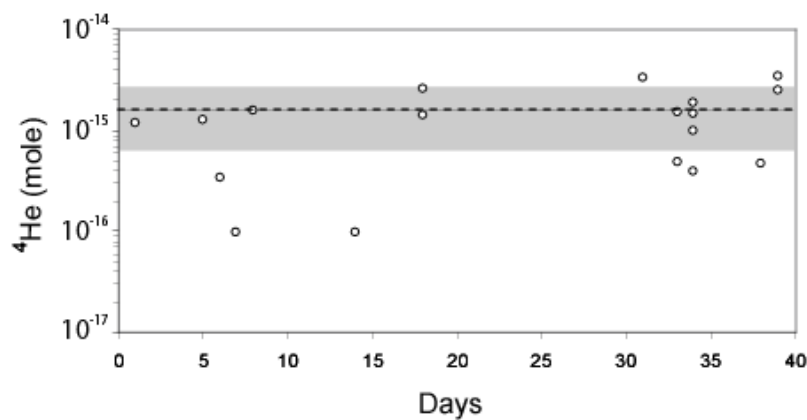
290

291 Figure 6: Evolution of the neon blanks as a function of the number of degassing  
292 cycles. A large amount of neon ( $> 10^{-14}$  mole  $^{20}\text{Ne}$ ) was degassed from the crucible  
293 and the hot ceramics during the first two cycles at around 1800°C. After two  
294 additional cycles at the same temperature, the blanks were stabilized at a low and  
295 acceptable level of  $\approx 5 \times 10^{-17}$  mole.

296

297 The helium blanks were measured at different temperatures with the furnace  
298 closed in static vacuum for 10 minutes. They are equal to  $1.84 \pm 1.58 \times 10^{-16}$  mole  
299  $^4\text{He}$  (n=5) at low temperature (1500°C) and  $1.64 \pm 1.03 \times 10^{-15}$  mole  $^4\text{He}$  (n=18) at  
300 1750°C.

301 We have tested the helium blank stability over a period of one month. Despite  
302 periodical exposures of the furnace to the atmosphere and sequential sample  
303 loading, we found that the blanks did not vary by more than 50-70% (Figure 7).



304  
305 Figure 7: Evolution of procedural  $^4\text{He}$  blanks over a period of 40 days. The dashed  
306 line represents the mean value ( $1.64 \times 10^{-15}$  mole  $^4\text{He}$ ) and the grey band indicates  
307 deviations of 50% relative to the mean value. This variability is comparable for the  
308 other noble gases. Following Stuart et al. (1999), we suspect that the He blanks may  
309 increase as a result of deformations of the bellow during opening and closing of the  
310 furnace valve. Part of the He blank may also be derived from helium diffusion through  
311 the pyrex viewport connected to the top CF200 flange.

312  
313 The neon blanks (with the furnace left for 20 minutes under static vacuum)  
314 were  $5.82 \pm 2.26 \times 10^{-17}$  mole  $^{20}\text{Ne}$  (n=7) at 1500°C and  $1.65 \pm 0.54 \times 10^{-16}$  mole  
315  $^{20}\text{Ne}$  (n=6) at 1600-1700°C, respectively. At temperatures below 1200°C, the neon

316 blanks were similar to those of the whole purification line, that is  $\sim 2.5 \times 10^{-17}$  mole  
317  $^{20}\text{Ne}$ .

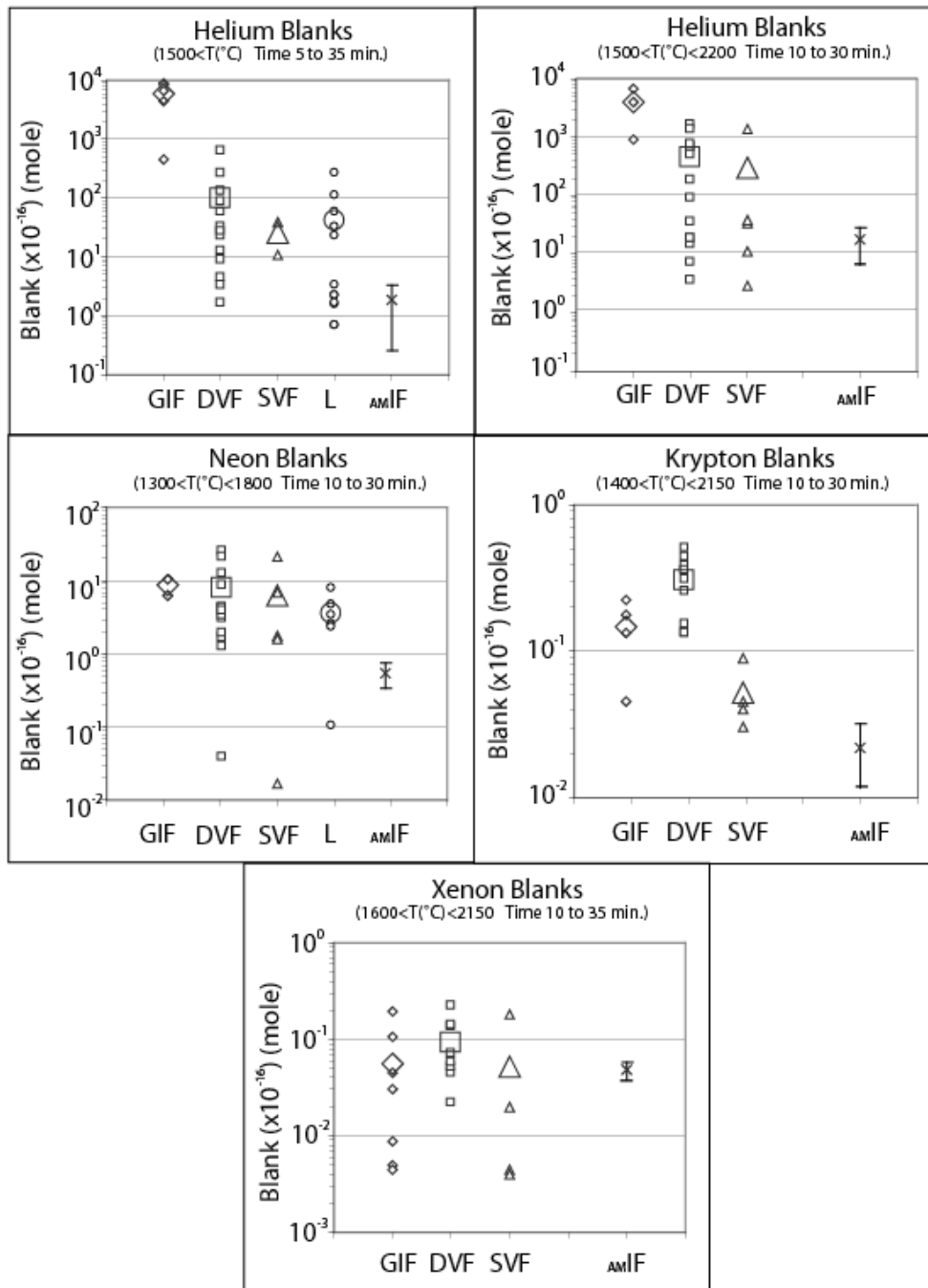
318

319 An analytical protocol of 10 minutes at high temperature in static vacuum has  
320 been applied to determine the heavy noble gas blanks. The amounts of  $^{84}\text{Kr}$   
321 degassed by the crucible were  $2.61 \pm 0.33 \times 10^{-19}$  mole at  $800^\circ\text{C}$  and  $2.13 \pm 0.29 \times$   
322  $10^{-18}$  mole at  $1700^\circ\text{C}$ . The xenon blanks, in the same range of temperature, were  
323  $4.45 \pm 0.42 \times 10^{-18}$  mole  $^{132}\text{Xe}$ .

324

325 Most samples are packed into a metallic foil before melting in the crucible.  
326 Although ideal to manipulate powders, this type of packaging is difficult to degas and  
327 chemical reactions between metallic foils and the Ta crucible might increase noble  
328 gas blanks upon heating (Niedermann et al. 1997). In order to determine the gas  
329 fraction derived from the metallic foils (Sn, Al), they were rolled to form a package  
330 similar to those containing the samples and analysed after baking at  $200^\circ\text{C}$  for 12  
331 hours. These analyses demonstrated that atmospheric noble gases were completely  
332 removed since He and Ne blanks were similar to those measured without a Sn or Al  
333 foil. The blanks of the heavy noble gases were systematically larger with metallic foils  
334 than without them. The krypton blanks were increased by a factor 4 in the range  
335  $800^\circ\text{C}$ - $1220^\circ\text{C}$ , and then by a factor 7 at  $1700^\circ\text{C}$ . The Xe blanks were stable until  
336  $1200^\circ\text{C}$  but then increased up to  $1.4 \times 10^{-17}$  mole  $^{132}\text{Xe}$  at  $1700^\circ\text{C}$ . We propose that  
337 the higher blanks result from the formation of alloys between the tantalum of the  
338 crucible and other metals from the foils, as already noted by **Niedermann et al.**  
339 **1997**, and observed under a binocular microscope.

340



341

342 Figure 8: Summary of the noble gas blanks measured with different heating methods:

343 glass induction furnaces (GIF; diamonds); double vacuum resistance furnaces (DVF,

344 open squares), simple vacuum resistance furnaces (SVF; triangle), lasers heating (L;

345 open circles) and the full-metal induction furnace presented here (amIF; cross). Large

346 symbols represent the average blank for each method. The all metal induction blanks

347 have been measured without melting metallic foils. Values and references are  
348 provided as supplementary material.

349

#### 350 4.1/ Comparison with other heating extraction methods

351

352 With our newly developed all-metal induction furnace, the blank amounts  
353 have been reduced by 60% to 99% for helium, neon and krypton when compared to  
354 those of others extraction methods such as glass induction furnaces (e.g. Ott 1988;  
355 Marty et al. 1995; Moreira & Allègre, 2002), double vacuum resistance furnaces (e.g.  
356 Niedermann et al 1997; Maruoka & Matsuda 2001; Blard et al. 2015), simple vacuum  
357 resistance furnaces (e.g. Honda et al. 1987; Burgess et al. 2009; Zimmermann et al.  
358 2012) and lasers (e.g. Stuart et al. 1999; Farley et al. 2006; Füre et al 2015). No clear  
359 improvement has been noted for xenon blanks with this new apparatus (Figure 8).

360

361 In double vacuum resistance furnaces, crucibles are heated by an electrical  
362 resistance which heats a tantalum liner (see for example Takaoka, 1976 and  
363 Staudacher et al. 1978). Extraction temperatures up to 1800°C can be achieved,  
364 resulting in blanks in the ranges of  $1.66 \times 10^{-16}$  -  $7.54 \times 10^{-14}$  mole  $^4\text{He}$ ,  $1.34 \times 10^{-16}$  -  
365  $2.68 \times 10^{-15}$  mole  $^{20}\text{Ne}$ ,  $3.0 \times 10^{-18}$  -  $5.13 \times 10^{-17}$  mole  $^{84}\text{K}$  and  $0.04 \times 10^{-17}$  -  $0.22 \times 10^{-16}$   
366 mole  $^{132}\text{Xe}$  (Figure 8). Lavielle et al. (1999) describe a similar double-walled  
367 vacuum furnace where the heat is produced by electron bombardment onto a Ta  
368 crucible, which has very low helium and neon blanks of  $1.78 \times 10^{-15}$  mole  $^4\text{He}$  and  
369  $0.04 \times 10^{-16}$  mole  $^{20}\text{Ne}$  respectively. This type of furnace has low blanks, but also has  
370 several drawbacks; first, the heating cycle of the sample is long because of a gradual  
371 and long increase of the temperature ( $<100^\circ\text{C}\cdot\text{min}^{-1}$ ) to protect the heating

372 components against electrical and thermal constraints. Furthermore, the Ta-tube is  
373 heavy (0.7 to 1 Kg), resulting in an important thermal inertia. Typical durations of  
374 temperature increase and decrease steps are about 20 min, potentially increasing  
375 the noble gas blanks. Second, this technology is costly since it requires expensive  
376 electrical resistances and thermal shields, a turbomolecular pumping system  
377 connected to the double vacuum vessel with yearly service and a regular  
378 replacement of the tantalum crucible after the melting of the samples ( $\approx 1500$   
379 €/crucible). Third, noble gases extracted from samples may be pumped by the  
380 external pumping system through cracks produced by the recrystallisation of the  
381 crucible walls after several heating cycles

382 Others furnaces have been developed in order to avoid a loss of gas through  
383 the crucible wall. In a simple vacuum resistance furnace, a W, or Ta, coil is heated by  
384 an electric current up to  $>2100^{\circ}\text{C}$  (Honda et al. 1987; Burgess et al. 2009; Sumino et  
385 al. 2011). As for the double vacuum furnaces, their use to extract noble gases is  
386 limited for several reasons: (i) they are not designed to be used with large samples  
387 because the inner volume of the coil is limited to a few  $\text{cm}^3$ ; (ii) all the samples must  
388 be packed into a metallic foil whose the degassing could increase the blanks  
389 (Niedermann et al. 1997); (iii) this metallic foil must remain in a solid state (without  
390 melting) during the extraction to avoid the loss of the sample through the coil wires.

391 Zimmermann et al. (2012) developed another design for a simple vacuum  
392 resistance furnace. The metal coil used by Honda et al. (1987) has been replaced by  
393 a Ta-resistance positioned around a boron nitride (BN) crucible. This furnace has  
394 satisfactory helium and neon blanks, but it is unable to melt refractory samples such  
395 as high-Mg olivines because its temperature is limited to  $\leq 1450^{\circ}\text{C}$ . Furthermore, it  
396 produces large amounts of nitrogen ( $>10^{-2}$  mbar) at high temperatures from BN,

397 which require extensive purification. In order to increase the lifetime of the resistance,  
398 it is recommended to respect a low heating rate around  $70^{\circ}\text{C}\cdot\text{min}^{-1}$ .

399 Farley et al. (1999) described a helium diffusion system developed specifically  
400 for He analyses. The samples are heated by radiation using a halogen lamp (250W).  
401 The He blanks are exceptionally low ( $1 - 4 \times 10^{-15}$  mole  $^4\text{He}$  at  $750^{\circ}\text{C}$ ), but its  
402 maximum temperature of  $800^{\circ}\text{C}$  to  $1000^{\circ}\text{C}$  limits the system to He diffusion  
403 experiments.

404 The induction furnaces using a glass vacuum vessel are sometimes used to  
405 extract noble gases from refractory samples such as olivine or barite (e.g. Becker &  
406 Pepin 1984; Ott 1988; Marty et al. 1995; Moreira & allègre 2002; Avice et al. 2015).  
407 Crucibles are heated by an external induction coil and the glass walls are cooled by  
408 water circulation. These furnaces can reach high temperatures ( $>1800^{\circ}\text{C}$ ) and their  
409 Ne, Kr and Xe blanks are similar to, or lower than, those of all-metal furnaces.  
410 Despite these interesting features, their use to extract gases is often challenging  
411 because (i) the heating rate to reach high temperatures is low,  $< 50^{\circ}\text{C}\cdot\text{min}^{-1}$ , in order  
412 to minimize thermal constraints on the crucible holder made of quartz; (ii) the volume  
413 of the crucible,  $< 3 \text{ cm}^3$ , is low; (iii) helium blanks are very high, generally  $> 9 \times 10^{-14}$   
414 mole  $^4\text{He}$  due to He diffusion through the pyrex or kovar vacuum envelope and (iv)  
415 neon blanks are also high, possibly due to degassing of the quartz screen.

416 Laser systems ( $\text{CO}_2$ , Nd-Yag, Diode) are also used to heat/melt mineral  
417 grains. They have the advantage of rapidly reaching high temperatures in excess of  
418  $2000^{\circ}\text{C}$ . They also yield low blanks: the furnace walls and the sample holders are  
419 moderately heated since the samples absorb most of the energy. However, the small  
420 sizes of the beams and their low power for most commercial instruments limit these  
421 devices to small sample sizes, typically below 10 mg. Further complication may arise

422 from vapor deposition onto the windows, or degradation of the latter by the laser  
423 beam.

424

425 5/ Noble gas extraction yields

426

427 Quartz, pyroxenes, olivine and barites samples have been analysed to  
428 determine the key parameters (temperature, grain size, duration) controlling the  
429 extraction efficiency. The results are given in the table 9A and 9B for He and Ne and  
430 Kr and Xe, respectively.

431 Helium was completely released by heating pyroxene and pyroxene-olivine at  
432 1750°C during 10 minutes. For pure refractory olivine, we nevertheless recommend  
433 to increase the temperature to 1770°C and the duration to 20 minutes in order to  
434 achieve complete extraction. 98% - 100% Ne was released from quartz of different  
435 grain size during the first step at 1500°C for 20 minutes. More than one hundred He  
436 and Ne analyses have been performed without any extraction problems and we did  
437 not observe a memory effect in the furnace for these gases.

438 Helium and neon were also analysed in pyroxenes (n=4) (CRONUS-P  
439 standard (Blard et al. 2015) and quartz (n=4) (CREU-1 standard (Vermeesch et al.  
440 2015) using the analytical protocol described above. The mean concentrations  
441 determined are  $5.01 \pm 0.12 \times 10^9$  atom  $^3\text{He.g}^{-1}$  and  $3.48 \pm 0.06 \times 10^8$  atom  $^{21}\text{Ne}$ ,  
442 consistent with the recommended values of  $5.02 \pm 0.12 \times 10^9$  atom  $^3\text{He.g}^{-1}$  and  
443  $3.48 \pm 0.10 \times 10^8$  atom  $^{21}\text{Ne}$ , respectively (Blard et al. 2015); (Vermeesch et al. 2015).  
444 This comparison further demonstrates the reliable noble gas extraction efficiency of  
445 our furnace.

446 Xe and Kr measurements of barite ( $\text{BaSO}_4$ , dissociation at  $1600^\circ\text{C}$ ) and quartz  
447 ( $\text{SiO}_2$ , decrepitation of fluid inclusions around  $1600^\circ\text{C}$ ) samples have also been  
448 conducted with this new furnace (Figure 9B). They consisted of two extractions steps  
449 at  $800^\circ\text{C}$  and  $1700^\circ\text{C}$ , and an additional re-extraction ("R" in Figure 9B) at a similar  
450 or slightly higher temperature ( $1750^\circ\text{C}$ ). Overall, 90 % of the gases were released  
451 during the first two steps, and 10% of the gases were extracted during the re-  
452 extraction steps. Noble gases extracted during this last step had an isotopic  
453 compositions close to those of the terrestrial atmosphere, probably due to an  
454 increase of the blank contribution.

455

Sample	Grain size ( $\mu\text{m}$ )	Mass (g)	Time (min.)	Temp. ( $^{\circ}\text{C}$ )	$^4\text{He}$ (mol)	$^{20}\text{Ne}$ (mol)	Extraction yield (%)
Pyrox. (100%)	125-250	0.160	10	1750	$6.40 \times 10^{-13}$		
R			10	1750	$9.77 \times 10^{-17}$		100.2
Pyrox. (50%)/ Ol. (50%)	125-250	0.109	10	1750	$2.78 \times 10^{-14}$		
R			10	1750	n.d.		100.00
Ol. (100%)	125-250	0.057	10	1750	$8.83 \times 10^{-14}$		
			10	1770	$2.08 \times 10^{-14}$		
R			10	1770	$1.59 \times 10^{-15}$		100.05
Quartz (100%)	100-400	0.314	20	1500		$7.84 \times 10^{-15}$	
R			20	1500		$9.76 \times 10^{-17}$	99.53
Quartz (100%)	400-1000	0.179	20	1500		$8.82 \times 10^{-15}$	
R			20	1500		$2.06 \times 10^{-16}$	98.35

458 Table 9A: Helium and neon extraction yield from pyroxene, olivine and quartz. Each values has been corrected for the blank  
 459 contributions, namely  $\sim 1.6 \times 10^{-15}$  mole  $^4\text{He}$  and  $5.8 \times 10^{-17}$  mole  $^{20}\text{Ne}$ . "R" denotes re-extraction.

Sample	Grain size ( $\mu\text{m}$ )	Mass (g)	Time (min.)	Temp. ( $^{\circ}\text{C}$ )	$^{84}\text{Kr}$ (mol)	Extraction yield ( $^{84}\text{Kr}$ ) (%)	$^{132}\text{Xe}$ (mol)	Extraction yield ( $^{132}\text{Xe}$ ) (%)
Barite	1000-3000	1.02	20	800	$1.5 \times 10^{-16}$	39.27	$1.60 \times 10^{-16}$	39.41
			20	1700	$1.8 \times 10^{-16}$	47.12	$2.0 \times 10^{-16}$	49.26
R			20	1700	$5.2 \times 10^{-17}$	13.61	$4.6 \times 10^{-17}$	11.33
Barite	1000-3000	0.87	20	800	$1.0 \times 10^{-16}$	64.52	$7.0 \times 10^{-17}$	45.75
			20	1700	$4.2 \times 10^{-17}$	27.10	$6.0 \times 10^{-17}$	39.22
R			20	1700	$1.3 \times 10^{-17}$	8.39	$2.3 \times 10^{-17}$	15.03
Quartz	1000-3000	0.92	20	800	$1.1 \times 10^{-15}$	67.07	$1.7 \times 10^{-15}$	59.65
			20	1700	$4.3 \times 10^{-16}$	26.22	$9.9 \times 10^{-16}$	34.74
R			20	1750	$1.1 \times 10^{-16}$	6.71	$16 \times 10^{-16}$	5.61

461

462 Figure 9B: Krypton and xenon extraction yield from barite and quartz. "R" denotes re-extraction.

463

## 464 6/ Conclusion

465

466 We have developed a new furnace design for noble gas extraction under ultra-  
467 high vacuum. A coil inside a full-metal single vacuum chamber is heating by induction  
468 a crucible located in the same chamber. This furnace can rapidly reach a  
469 temperature of at least 1850°C within only few minutes (heating/cooling rates of  
470 about 400°C.min<sup>-1</sup>), thanks to its low thermal inertia and its assemblage that prevents  
471 degradation by thermal shocks. The whole furnace and the sample holder (carrousel)  
472 can be baked at 200°C for several days. The chamber envelope and upper/lower  
473 flanges are cooled down by a water circulation during heating, warranting very low  
474 noble gas blanks compared to existing furnaces.

475 Future tests will focus on: (i) testing new crucibles with low Ar blanks in order  
476 to be able to analyse this noble gas in geological samples; (ii) adding a thermocouple  
477 or a new optical pyrometer to have a more rigorous control of the temperature  
478 especially in the 100 - 900 °C temperature range; (iii) testing Pt crucibles for  
479 quantitatively extracting nitrogen together with noble gases.

480 A patent of this new furnace has been issued to the Institut National de la  
481 Propriété Industrielle. Its marketing mode will be ensured by the society Cryoscan.

482

## 483 Acknowledgments

484 This research was supported by funding from Otelio. The CRPG contribution is  
485 XXXX.

486

## 487 References

488

489 **Aciego S.M., DePaolo D.J., Kennedy B.M., Lamb M.P., Sims K.W.W. and Dietrich**  
490 **W.E. (2007)**

491 Combining [3He] cosmogenic dating with U-Th/He eruption ages using olivine in  
492 basalt. . Earth and Planetary Science Letters, **254**, 288-302

493

494 **Avice G., Meier M.M.M., Marty B., Wieler R., Kramers J.D., Langenhorst F.,**  
495 **Cartigny P., Maden C., Zimmermann L., Andreoli M.A.G., (2015).**

496 A comprehensive study of noble gases and nitrogen in “Hypatia,” a diamond-rich  
497 pebble from SW Egypt. Earth and Planetary Science Letters, **432**, 243–253

498

499 **Ammon K., Dunai T.J., Stuart F.M., Meriaux A.-S. and Gayer E. (2009)**

500 Cosmogenic 3He exposure ages and geochemistry of basalts from Ascension Island,  
501 Atlantic Ocean. Quaternary Geochronology, **4**, 525-532

502

503 **Becker R.H. and Pepin R.O. (1984)**

504 The case for a martian origin of the shergottites: nitrogen and noble gases in EETA  
505 79001. Earth and Planetary Science Letters, **69**, 225-242

506

507 **Blard P.H., Pik R., Lavé J., Bourlès D., Burnard P.G., Yokochi R., Marty B. and**  
508 **Trusdell (2006)**

509 Cosmogenic 3He production rates revisited fom evidences of grain size dependent  
510 release of matrix-sited helium. Earth and Planetary Science Letters, **247**, 222-234

511

512 **Blard P.H. and Pik R. (2008)**

513 An alternative isochron method for measuring cosmogenic  $^3\text{He}$  in lava flows.  
514 Chemical Geology, **251**, 20-32

515

516 **Blard P.H., Braucher R., Lavé, J. and Bourlès, D., (2013)**

517 Cosmogenic  $^{10}\text{Be}$  production rate calibrated against  $^3\text{He}$  in the high Tropical Andes  
518 (3800–4900 m, 20–22° S). Earth and Planetary Science Letters, **382**, 140–149

519

520 **Blard P. H., Lave, J., Farley K. A., Ramirez V., Jimenez N., Martin L. C., Charreau  
521 J., Tibari B. and Fornari M. (2014).**

522 Progressive glacial retreat in the Southern Altiplano (Uturuncu volcano, 22° S)  
523 between 65 and 14ka constrained by cosmogenic  $^3\text{He}$  dating. Quaternary  
524 Research, **82**(1), 209-221.

525

526 **Blard P.H., Balco G., Burnard P.G., Farley K.A., Fenton C.R., Friedrich R., Jull  
527 A.J.T., Niedermann S., Pik R., Schaefer J.M., Scott E.M., Shuster D.L., Stuart  
528 F.M., Stute M., Tibari B., Winckler G. and Zimmermann L. (2015)**

529 An inter-laboratory comparison of cosmogenic  $^3\text{He}$  and radiogenic  $^4\text{He}$  in the  
530 cronus-P pyroxene standard. Quaternary Geochronology, **26**, 11-19

531

532 **Burgess R., Cartigny P., Harrison D., Hobson E. and Harris J. (2009)**

533 Volatile composition of microinclusions in diamonds from the panda kimberlite,  
534 Canada: Implications for chemical and isotopic heterogeneity in the mantle.  
535 Geochimica et Cosmochimica Acta, **73**, 1779-1794

536

537 **Chennaoui-Aoudjehane H. (1992)**

538 Modélisation de la solubilité des gaz rares He, Ne, Ar, Kr et Xe dans les liquides  
539 silicatés à 1500°C. Thèse 138 p

540

541 **Chiggiato P., Benvenuti C., Canil G., Collin P., Cosso R., Guerin J. and Ilie S.**  
542 **(1999)**

543 Surface cleaning efficiency measurements for UHV applications. Vacuum, **53**, 317-  
544 320

545

546 **Farley K.A., Libarkin J., Mukhopadhyay S. and Amidon W. (2006)**

547 Cosmogenic and nucleogenic  $^3\text{He}$  in apatite, titanite, and zircon. Earth and Planetary  
548 Science Letters, **248**, 451-461

549

550 **Foeken J.P.T., Stuart F.M., Dobson K.J., Persano C. and Vilbert D. (2006)**

551 A diode laser system for heating minerals for (U-Th)/He chronometry. Geochemistry  
552 Geophysics Geosystems, Technical brief, **7**, Q04015

553

554 **Foeken J.P.T., Day S. and Stuart F.M. (2009)**

555 Cosmogenic  $^3\text{He}$  exposure dating of the quaternary basalt from Fogo, Cape Verdes:  
556 Implications for tift zone and magmatic reorganisation. Quaternary Geochronology, **4**,  
557 37-49

558

559 **Füri E., Aléon-Toppani A., Marty B. and Libourel G. (2013)**

560 Effects of atmospheric entry heating on the noble gas and nitrogen content of  
561 micrometeorites. Earth and Planetary Science Letters, **377-378**, 1-12

562

563 **Füri E., Chaussidon M. and Marty B. (2015)**

564 Evidence for an early nitrogen isotopic evolution in the solar nebula from volatile  
565 analyses of a CAI from the CV3 chondrite NWA 8616. *Geochimica et Cosmochimica*  
566 *Acta*, **153**, 183-201

567

568 **Honda M., Reynolds J.H., Roedder E. and Epstein S. (1987)**

569 Noble gases in diamonds: Occurrences of solarlike helium and neon. *Journal of*  
570 *Geophysical Research*, **92**, N°B12, 12.507-12521

571

572 **Honda M., Mcdougall I, Patterson D.B., Doulgeris A. and Clague D.A. (1993)**

573 Noble gases in submarine pillow basalt glasses from Loihi and Kilauea, Hawaii: A  
574 solar component in the Earth. *Geochimica et Cosmochimica Acta*, **57**, 859-874

575

576 **Jambon A., Weber H. and Braun O. (1986)**

577 Solubility of He, Ne, Ar, Kr and Xe in a basalt melt in the range 1250-1600°C.  
578 Geochemical implications. *Geochimica et Cosmochimica Acta*, **50**, 401-408

579

580 **Johnson L.H., Burgess R., Turner G., Milledge H.J. and Harris J.W. (2000)**

581 Noble gas and halogen geochemistry of mantle fluids: Comparison of african and  
582 canadian diamonds. *Geochimica et Cosmochimica Acta*, **64**, 717-732

583

584 **Kurz M. (1986)**

585 In situ production of terrestrial cosmogenic helium and some application to  
586 geochronology. *Geochimica et Cosmochimica Acta*, **50**, 2855-2862

587

588 **Lavielle B., Marti K., Jeannot J.P., Nishiizumi K. and Caffee M. (1999)**  
589 The  $^{36}\text{Cl}$ - $^{36}\text{Ar}$ - $^{40}\text{K}$ - $^{41}\text{K}$  records and cosmic ray production rates in iron meteorites.  
590 Earth and Planetary Science Letters, **170**, 93-104  
591

592 **Marty B, Lenoble M. and Vassard N. (1995)**  
593 Nitrogen, helium and argon in basalt: a static mass spectrometry study. Chemical  
594 Geology (Isotope Geoscience Section), **120**, 183-195  
595

596 **Maruoka T. and Matsuda J. (2001)**  
597 New crucible for noble gas extraction. Chemical Geology, **175**, 751-756  
598

599 **Moreira M. and Allègre C.J. (2002)**  
600 Rare gas systematics on Mid Atlantic Ridge (37-40°N). Earth and Planetary Science  
601 Letters, **198**, 401-416  
602

603 **Nichols R. H. Jr., Hohenberg C.M. and Olinger C.T. (1994)**  
604 Implanted solar helium, neon, and argon in individual lunar ilmenite grains: Surface  
605 effects and a temporal variation in the solar wind composition. Geochimica et  
606 Cosmochimica Acta, **58**, 1031-1042  
607

608 **Niedermann S., Bach W. and Erzinger J. (1997)**  
609 Noble gas evidence for a lower mantle component in MORBs from the southern East  
610 Pacific Rise: Decoupling of helium and neon isotope systematics. Geochimica et  
611 Cosmochimica Acta, **61**, 2697-2715  
612

613 **Ott U. (1988)**

614 Noble gases in SNC meteorites: Shergotty, Nakhla, Chassigny. *Geochimica et*  
615 *Cosmochimica Acta*, **52**, 1937-1948

616

617 **Ozima M., Podosek, F.A. (2002)**

618 Noble Gas Geochemistry, Second Edition. ed. Cambridge University Press,  
619 Cambridge.

620

621 **Persano C., Stuart F.M., Bishop P. and Barfod D.N.**

622 Apatite (U-Th)/He age constraints on the development of the great escarpment on  
623 the southeastern Australian passive margin. *Earth and Planetary Science Letters*,  
624 **200**, 79-90

625

626 **Pi T., Solé J. and Taran Y. (2005)**

627 (U-Th)/He dating of fluorite: application to the La Azul fluorite deposit in the Taxco  
628 mining district, Mexico. *Mineralium Deposita*, **39**, 976-982

629

630 **Pujol M., Marty B., Burnard P., Philippot P., 2009.**

631 Xenon in Archean barite: Weak decay of  $^{130}\text{Ba}$ , mass-dependent isotopic  
632 fractionation and implication for barite formation. *Geochimica et Cosmochimica Acta*  
633 **73**, 6834–6846.

634

635 **Staudacher Th, Jessberger E.K., Dörflinger D. and Kiko J. (1978)**

636 A refined ultrahigh-vacuum furnace for rare gas analysis. *J. Phys. E: Sci. Instrum*, **11**,  
637 781-784

638

639 **Stuart F.M., Harrop P.J., Knott S. and Turner G. (1999)**

640 Laser extraction of helium isotopes from Antarctic micrometeorites: Source of He and  
641 implications for the flux of extraterrestrial  $^3\text{He}$  to earth. *Geochimica et Cosmochimica*  
642 *Acta*, **63**, 2653-2665

643

644 **Sumino H., Dobrzhinetskaya L.F., Burgess R. and Kagi H. (2011)**

645 Deep-mantle-derived noble gases in metamorphic diamonds from the Kokchetav  
646 massif, Kazakhstan. *Earth and Planetary Science Letters*, **307**, 439-449

647

648 **Vermeesch P., Balco G., Blard P. H., Dunai T. J., Kober F., Niedermann S.,**

649 **Shuster D. L., Strasky S., Stuart F. M., Wieler R. and Zimmermann L. (2015)**

650 Interlaboratory comparison of cosmogenic  $^{21}\text{Ne}$  in quartz. *Quaternary*  
651 *Geochronology*, **26**, 20-28

652

653 **Williams A.J., Stuart F.M., Day S.J. and Phillips W.M. (2005)**

654 Using pyroxene microphenocrysts to determine cosmogenic  $^3\text{He}$  concentrations in  
655 old volcanic rocks; an example of landscape development in central Gran Canaria.  
656 *Quaternary Science Reviews*, **24**, 211-222

657

658 **Wieler R. (2014)**

659 Noble Gas Mass Spectrometry, in: *Treatise on Geochemistry (Second Edition)*.  
660 Elsevier, Oxford, pp. 355–373.

661

662 **Yokochi R. and Marty B. (2006)**

663 Fast chemical and isotopic exchange of nitrogen during reaction with hot  
664 molybdenum. *Geochemistry Geophysics Geosystems*, Technical brief, **7**, Q07004  
665  
666 Supplementary

<i>Autor(s)</i>	<i>Laboratories</i>	<i>Crucible</i>	<i>Temperature</i>	<sup>4</sup> He (mole) (x10 <sup>-16</sup> )	<sup>20</sup> Ne (mole) (x10 <sup>-16</sup> )	<sup>84</sup> Kr (mole) (x10 <sup>-16</sup> )	<sup>132</sup> Xe (mole) (x10 <sup>-16</sup> )
<b>Glass Induction Furnace</b>							
Becker & Pepin (1984)	Univ. of Minesota		1500	4461 <sup>(-)</sup>	6.69 <sup>(-)</sup>	0.134 <sup>(-)</sup>	0.004 <sup>(-)</sup>
				6692 <sup>(+)</sup>	11.15 <sup>(+)</sup>	0.223 <sup>(+)</sup>	0.009 <sup>(+)</sup>
CRPG (unpublished data)	CRPG	Ta	1800				0.031
			2200				0.045
Marty et al. (1995)	Magie	Mo	600	460			
			1800	900			
Moreira & Allègre (2002)	IPGP	Mo	600	8923	4.46	0.054	0.005
			1500	8477	6.69	0.045	0.005
Pujol (2009)	CRPG	Ta	1850				0.194
Ott (1988)	Max Planck Institut	Mo	1600	6692	11.15	0.178	0.107
<b>Double Vacuum Furnace</b>							
Aciego et al. (2007)	Berkeley	-	300-1500	22.31 <sup>(-)</sup>			
				58.00 <sup>(+)</sup>			
Blard & Pik (2008)	CRPG	Ta	1600	88.04			
Blard et al. (2015)	GFZ Potsdam	Ta	900	1.66 <sup>(-)</sup>			
				3.32 <sup>(+)</sup>			
	GFZ Potsdam	Ta	1750	6.64 <sup>(-)</sup>			
				33.22 <sup>(+)</sup>			
	Latmont, Palissades	Mo	1350	33.22			
	Caltech, Pasadena	-	1500	26.58			
Foeken et al. (2009)	Scottish Universities	-	1300	12.46			
Honda et al. (1993)	Australian National University	Ta	600-1500	133.84	1.75	0.134	0.022
		Al <sub>2</sub> O <sub>3</sub>	600-1500	267.69	26.29		
Jambon et al. (1986)	Max Planck Institut	Mo	1650	178.46	26.77	0.357	0.223
Kurz (1986)	Woods Hole oceanographic Institution		-	13.38 <sup>(-)</sup>			
			-	17.85 <sup>(+)</sup>			
Lavielle et al. (1999)	Univ. of Bordeaux I	-	1750-1800	17.85	0.04		
Maruoka & Matsuda (2001)	University of Vienna	MgO	800	642.46			
		MgO	1600	660.30	3.30 <sup>(x)</sup>	0.261 <sup>(x)</sup>	0.072 <sup>(x)</sup>
		BN	600-800	-	3.39 <sup>(x)</sup>	0.254 <sup>(x)</sup>	0.020 <sup>(x)</sup>
		BN	1600	481.84	3.53 <sup>(x)</sup>	0.513 <sup>(x)</sup>	0.045 <sup>(x)</sup>
		BN	1800	1548*	4.04 <sup>(x)</sup>	0.388 <sup>(x)</sup>	0.052 <sup>(x)</sup>
		Mo	1600	753.99*	4.50 <sup>(x)</sup>	0.362 <sup>(x)</sup>	0.140 <sup>(x)</sup>
		Mo	1800	1307	9.20 <sup>(x)</sup>	0.154 <sup>(x)</sup>	0.058 <sup>(x)</sup>
Niedermann et al. (1997)	GFZ Potsdam	Ta	400-800	89.23			
			1400	89.23	4.46 <sup>(-)(2x)</sup>		
			1400	89.22	13.38 <sup>(+)(2x)</sup>		
					1.34 <sup>(-)(3x)</sup>		
					4.02 <sup>(+)(3x)</sup>		
Persano et al. (2002)	-		950	4.46 <sup>(4x)</sup>			
Vermeesch et al. (2015)	ETH Zurich		1750		2.01		
Williams et al. (2006)	SCUERC		1700	3.32 <sup>(4x)</sup>			
<b>Single Vacuum Furnace</b>							
Blard et al. (2006)	CRPG		1700	9.97 <sup>(-)</sup>			
				31.56 <sup>(+)</sup>			
				39.87 <sup>(5x)</sup>			
Blard et al. (2015)	CRPG	BN	1400				
Burgess et al. (2009)	University of Manchester	Ta coil	2150			0.089	0.178
Honda et al. (1987)	University of California	W coil	2000	1338	21.86	0.045	0.004
Johnson et al. (2000)	University of Manchester		1600			0.030	0.004

Sumino et al. (2011)	University of Tokyo	Ta coil	2050			0.040	0.020
			2200	2.68 <sup>(-)</sup>	0.02 <sup>(-)</sup>		
				35.69 <sup>(+)</sup>	7.14 <sup>(+)</sup>		
Zimmermann et al. (2012)	CRPG	BN	1450	11			
<b>Laser System</b>							
Ammon et al. (2009)	University of Edinburgh	808 nm		0.67 <sup>(-)</sup>			
				1.52 <sup>(+)</sup>			
Blard et al. (2015)	SUERC	808 nm	1400	1.66 <sup>(-)</sup>			
				3.32 <sup>(+)</sup>			
Farley et al. (2006)	California Institute of technology	Nd-Yag	1300	33.22			
Foeken et al. (2006)	SUERC	808 nm		0.67			
Foeken et al. (2009)	SUERC	808 nm	> 1200	2.16			
Füri et al. (2013)	CRPG	CO <sub>2</sub>		260	5.00		
				23.00	3.50		
Füri et al. (2015)	CRPG	CO <sub>2</sub>			2.45		
Nichols et al. (1994)	Washington University	Nd-Yag		111.54	0.11		
Pi et al. (2005)	University of Mexico	CO <sub>2</sub>		60			
Stuart et al. (1999)	SUERC	Nd-Yag		2.23	2.62		
Vermeesch et al. (2015)	ETH Zurich	810 nm			8.30		
<b>This study</b>							
	CRPG	Ta	1500	1.84 <sup>(x)</sup>			
	CRPG	Ta	1750	16.4 <sup>(x)</sup>			
	CRPG	Ta	1500		0.58 <sup>(x)</sup>		
	CRPG	Ta	1700			0.021 <sup>(x)</sup>	0.048 <sup>(x)</sup>

667

668 (x): Average of the blanks, For CRPG, x=3, 13, and 7 for He blank (1500°C), He blank  
669 (1750°C) and Ne, Kr & Xe blank respectively;

670 (-)(+): minimal and maximal value given in manuscript;

671 (2x)(3x)(4x)(5x) denote blanks measured after the Ni, Al, Cu and Sn foil melting  
672 respectively.

673 Analytical protocol for CRPG blanks: 10 min in static vacuum at high temperature for  
674 He and 20 min for Ne, Kr and Xe.

675